# Polarity-dependent pinning of a surface state

M. Schnedler,[1] V. Portz,[1] H. Eisele,[2] R. E. Dunin-Borkowski,[1] and Ph. Ebert[1,*]
[1]*Peter Grünberg Institut, Forschungszentrum Jülich GmbH, 52425 Jülich, Germany*
[2]*Institut für Festkörperphysik, Technische Universität Berlin, Hardenbergstraße 36, 10623 Berlin, Germany*
(Received 9 December 2014; revised manuscript received 22 April 2015; published 18 May 2015)

We illustrate a polarity-dependent Fermi level pinning at semiconductor surfaces with chargeable surface states within the fundamental band gap. Scanning tunneling spectroscopy of the GaN $(10\bar{1}0)$ surface shows that the intrinsic surface state within the band gap pins the Fermi energy only at positive voltages, but not at negative ones. This polarity dependence is attributed to arise from limited electron transfer from the conduction band to the surface state due to quantum mechanically prohibited direct transitions. Thus, a chargeable intrinsic surface state in the band gap may not pin the Fermi level or only at one polarity, depending on the band to surface state transition rates.

DOI: 10.1103/PhysRevB.91.205309 PACS number(s): 73.20.−r, 68.37.Ef

Chargeable electronic states at semiconductor interfaces, with energies inside the fundamental band gap, commonly induce a phenomenon known as Fermi level pinning [1]. These states can arise from the interface bonding structure of the semiconductor with, e.g., a metal (so-called metal-induced gap states) [2], or originate from the broken periodicity and the resulting dangling bonds at a semiconductor-vacuum surface [3]. At high densities these surface states may accommodate large quantities of surface charges, which effectively shield the underlying semiconductor from electric potentials applied at the surface (e.g., by metal contacts). The screening shifts the semiconductor's bands and aligns the Fermi level with the energy of the surface states (so-called Fermi level pinning). This effect influences the charge transport across the surface or interface and thus the Fermi level pinning phenomenon is of critical importance for semiconductor-based devices and nanostructures [4].

It is commonly understood that at sufficiently high densities of surface states in the order of $\approx 6\times10^{14}$ cm$^{-2}$ (corresponding to intrinsic surface states), the Fermi level pinning is essentially independent of the doping as well as of the polarity of externally applied electric fields [1,5]. This *equilibrium* model assumes a free charge transfer between bands and surface states. In this paper we illustrate that surfaces with chargeable surface states within the fundamental band gap can exhibit a polarity-dependent pinning, since the rate of electron transfer between the bands and surface states is too small due to quantum mechanically prohibited transitions. This leads to a one-sided, polarity-dependent Fermi level pinning, which by itself can create a rectifying behavior.

In order to demonstrate this effect, we use a semiconductor-vacuum-metal tip configuration in a scanning tunneling microscope as the model system. Scanning tunneling microscopy (STM) and spectroscopy (STS) is one of the few experimental methods to probe empty and filled surface states in a single experiment [6,7]. The tunnel current is highly sensitive to the band edge positions, providing direct access to the surface potential and hence to the Fermi level pinning [8–10]. Furthermore, the metallic tip of the STM can be used to apply electric fields, in order to probe the Fermi level pinning as a function of the magnitude and polarity of the applied field.

As semiconductor, we investigate the clean GaN$(10\bar{1}0)$ surface, since most tetrahedrally coordinated nonpolar compound semiconductor surfaces can be expected to behave similarly. Nonpolar compound semiconductor cleavage surfaces typically have one occupied anion-derived and one empty cation-derived dangling-bond surface state. If these surface states are shifted energetically into the bulk bands, as, e.g., for GaAs(110) [11], the tunneling spectroscopy seems to be rather well understood [7,12–14]. In contrast, for GaN$(10\bar{1}0)$ the energetic position of the empty surface state was controversially debated [15], since the initial STS experiments [16,17] and calculations [17,18] found no surface state within the fundamental band gap. However, recent calculations [19–22] as well as STS experiments at very small tip-sample separations revealed a "*hidden*," intrinsic empty surface state within the fundamental band gap, which has a very small spatial extension into the vacuum [23]. Hence, we use GaN$(10\bar{1}0)$ as an example of the group of compound semiconductors, whose nonpolar cleavage surfaces have an intrinsic surface state in the fundamental band gap.

For the experiments we cleaved *n*-type GaN layers (carrier concentration of $3\times10^{18}$ cm$^{-3}$) grown epitaxially by metal-organic chemical-vapor deposition on a freestanding GaN(0001) substrate. In order to improve the cleavage, $2\times6$ mm$^2$-sized samples (long axis in $\langle10\bar{1}0\rangle$ direction) were thinned to 100 $\mu$m thickness. Their bottom half is electrically contacted on both sides by sputtered Au contacts and mounted into the sample holder. The cleavage is initiated by pushing and cleaving off the upper (noncontacted) freestanding part of the samples in ultrahigh vacuum ($1\times10^{-8}$ Pa) to obtain contamination free and clean GaN$(10\bar{1}0)$ surfaces.

The cleavage surfaces consisted of large atomically flat terraces (see inset in Fig. 1), separated by steps. The steps were found to arise frequently from dislocations or stacking faults in the material [24,25]. STM images reveal that the GaN$(10\bar{1}0)$ cleavage surfaces used for the experiments have a low defect concentration. Thus, *no* relevant concentrations of *extrinsic* surface states and hence no *extrinsic* pinning can be expected. However, the surface should be *intrinsically* pinned due to the empty surface state in the fundamental band gap [22,23,26].

*p.ebert@fz-juelich.de

 

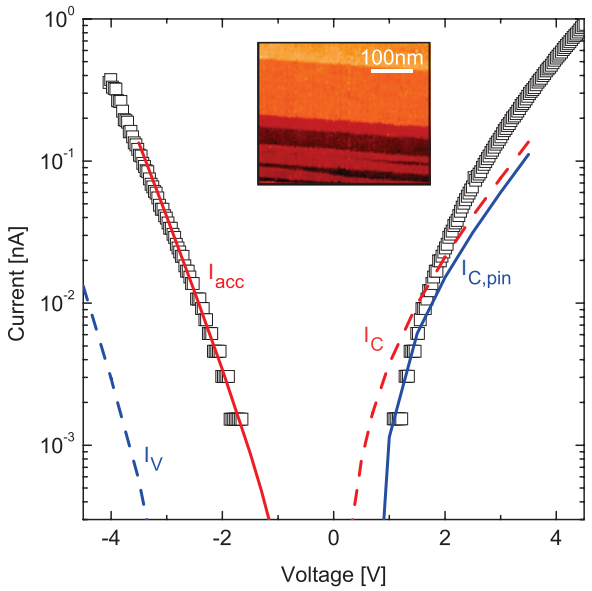


FIG. 1. (Color online) Scanning tunneling spectroscopy of the *n*-type GaN$(10\bar{1}0)$ surface at 290 K. The squares show the experimental data measured at a tip-sample separation fixed by a set voltage of −3.6 V and a set current of 150 pA. The lines represent calculations of the tunnel current with no intrinsic surface state in the band gap (red solid and dashed lines) and with an empty surface state at $E_C - 0.7$ eV (blue solid and dashed lines), pinning the Fermi energy. Inset: STM image of the GaN $(10\bar{1}0)$ surface, on which the spectrum was measured.

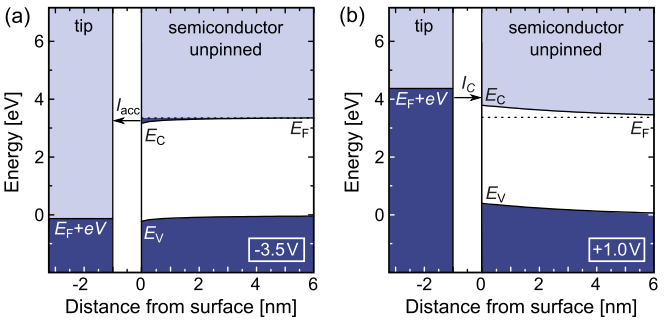


FIG. 2. (Color online) Calculated valence ($E_V$) and conduction ($E_C$) band edge positions for unpinned GaN surfaces with no surface states in the band gap for (a) negative (−3.5 V) and (b) positive (+1.0 V) voltages applied to the semiconductor sample. The sample is on the right side at positive distance values. The Fermi energy $E_F$ is close to the conduction band in the bulk. The tip with its Fermi energy at $E_F + eV$ is shown on the left-hand side. The dark blue (light blue) areas represent filled (empty) states. The band gap and the vacuum gap (tunnel barrier) between the surface at zero position (0 nm) and the tip position (at −1.06 nm) are shown in white. At negative voltages (a) the downward band bending induces an accumulation of electrons in the conduction band. These accumulated electrons tunnel into the tip resulting in an accumulation current $I_{acc}$. At positive voltages (b) the electrons tunnel from the tip into the conduction band states ($I_C$).

On this basis we turn to measured spectra. The tunneling spectrum in Fig. 1 shown as black squares exhibits a tunnel current branch at positive and negative voltages and a region in between with no detectable tunnel current (noise level ≈2 pA). The current onset voltages are about +1 V and −1.5 V, respectively. The voltage range without tunnel current arises from the existence of a band gap [12]. In this experiment, the voltage range without tunnel current ($\times e$) is significantly smaller than the bulk band gap of ≈3.4 eV. Furthermore, the onset voltage of +1 V is significantly larger than that of other *n*-type nonpolar compound semiconductor surfaces, for which values down to almost 0 V are typical [14,27]. Note, we found the same features, i.e., onset voltages and apparent band gap, in tunneling spectra measured on hydride vapor phase epitaxy grown GaN$(10\bar{1}0)$ cleavage surfaces as well as in published spectra in the literature [17,23]. Hence, the shown spectrum is representative and well reproducible.

In order to evaluate the measured tunneling spectra, we turn to a short qualitative discussion before continuing with a detailed numerical simulation. First, if a surface is fully *pinned* due to the presence of an intrinsic surface state in the band gap, the voltage range without current ($\times e$) corresponds exactly to the fundamental band gap [28]. This is visibly not observed here. Hence, the surface cannot be considered to be fully pinned. In contrast, for an *unpinned* surface, the electric field between the tip and the semiconductor sample induces a band bending in the semiconductor. At negative voltages, the downward band bending shifts the conduction band edge $E_C$ below the Fermi energy $E_F$ and thereby leads to a tip-induced electron accumulation in the conduction band [Fig. 2(a)]. The accumulated electrons can already tunnel at voltages within the band gap (accumulation current $I_{acc}$) and hence the voltage range without tunnel current is reduced [12,25,27]. Thus, at first view the tunneling spectrum can be explained apparently assuming an unpinned GaN surface despite the proven presence of an intrinsic surface state in the band gap [23,26].

However, this conclusion is in conflict with the current onset at positive voltages: For unpinned *n*-type surfaces of all other previously investigated compound semiconductor materials, the onset of the tunnel current at positive voltages is always found close to 0 V [14,27,29]. This should also be the case for unpinned GaN surfaces (as calculated below). This is well below the value of about +1 V observed here and visible in published tunneling spectra of *n*-type GaN$(10\bar{1}0)$ surfaces [16,17,23].

Thus, neither the model of an *unpinned* nor of a *pinned* surface can satisfactorily explain the experimental data.

To resolve this puzzling situation we turn to simulations of the tunnel current, in order to evaluate the measured tunneling spectrum quantitatively. The simulations of the tunnel current assume two different physical models: an *unpinned* and a *fully pinned* GaN surface.

We use a three-dimensional finite difference calculation of the electrostatic potential in a tip-vacuum-semiconductor sample system. In order to improve the accuracy we not only solve the Poisson equation for the electrostatic potential, but in addition, the continuity equations for holes and electrons [30]. Note, if we use the code of Feenstra solving the Poisson equation only [31], we obtain the same physical conclusions. Here we chose to include the continuity equations, since this is a more elaborate physical model, especially suited

to calculate the accumulation current. For the fully pinned surface, the intrinsic empty surface state is modeled as a Gaussian distribution 0.7 eV below the conduction band edge (FWHM = 0.1 eV) and a concentration of $6\times10^{14}$ cm$^{-2}$ following band-structure calculations [23]. The charge neutrality level at the surface $E_{\mathrm{CNL}}$ is chosen to be between the filled and empty intrinsic surface states [3]. The tunnel current is calculated using the potential distribution following Ref. [12]. The resulting tunnel currents are shown in Fig. 1 as solid and dashed lines. The corresponding band edge positions as a function of the distance into the sample through the central axis of the tip are shown in Figs. 2 and 3 for the unpinned and pinned surfaces, respectively.

First, we focus on the *unpinned* surface without surface states (red solid and dashed lines in Fig. 1):

(i) At negative voltages, the accumulation current $I_{\mathrm{acc}}$, consisting of electrons extracted from the electron accumulation zone in the conduction band [Fig. 2(a)], fits well to the experimental data for a tip-sample separation $z$ of 1.06 nm (compare the red solid line with symbols in Fig. 1). $z$ is the only fitting parameter used and is kept constant for all further calculations. Note, we used a slightly larger $z$ in the experiment to avoid tip-sample interactions and obtain more stable tunneling conditions.

(ii) At positive voltages, the tunnel current arises from tunneling of electrons into the empty conduction-band states [Fig. 2(b)]. The onset voltage of this calculated current is found close to +0.2 V ($I_{\mathrm{C}}$, red dashed line in Fig. 1). This does not describe the large experimentally observed onset voltage of about +1.0 V. In addition, the slope of the experimental data is not reproduced and at small voltages the calculated current is too large. Thus, the physical model of an unpinned surface only describes the spectrum at negative voltages properly.

Second, we address the *fully pinned* surface with an intrinsic surface state in the band gap as depicted in Fig. 3(a): For this pinned surface we discuss the effect of the proximity of the tip and an additional applied voltage.

(i) At positive voltages, the calculated current arises from electrons tunneling into the empty conduction band states ($I_{\mathrm{C,pin}}$, solid blue line in Fig. 1). The best fit yields an onset voltage now shifted to +0.81 V, in good agreement with the experimental onset voltage of about +1 V. In addition, the slope of the calculated current fits well to the experimental data at small positive voltages. The shifted onset voltage and the larger slope arise from the band bending being increased by $\Delta E$ as compared to the case without pinning [compare the band edge positions shown as dashed and solid lines in Fig. 3(c)]. With increasing positive voltage, the calculated tunnel current with (pinned, $I_{\mathrm{C,pin}}$) and without (unpinned, $I_{\mathrm{C}}$) intrinsic surface state increasingly merge. This effect is due to the change in electron occupation of the surface state with band bending: At *large* positive voltages, the surface state is energetically located fully above the Fermi energy and hence completely empty. Therefore, there is effectively no pinning of the Fermi level. In contrast, at *small* positive voltages, the tail of the surface state below the Fermi energy is occupied and the Fermi level is pinned.

(ii) At negative voltages, the pinning-induced upward band bending suppresses an electron accumulation in the conduction band [Fig. 3(b)]. Hence, only electrons from the valence band can tunnel into the tip. This valence band current $I_{\mathrm{V}}$ is too small (blue dashed line in Fig. 1).

Tunneling in or out of the intrinsic Ga-derived surface state in the band gap can be neglected, since its density of states

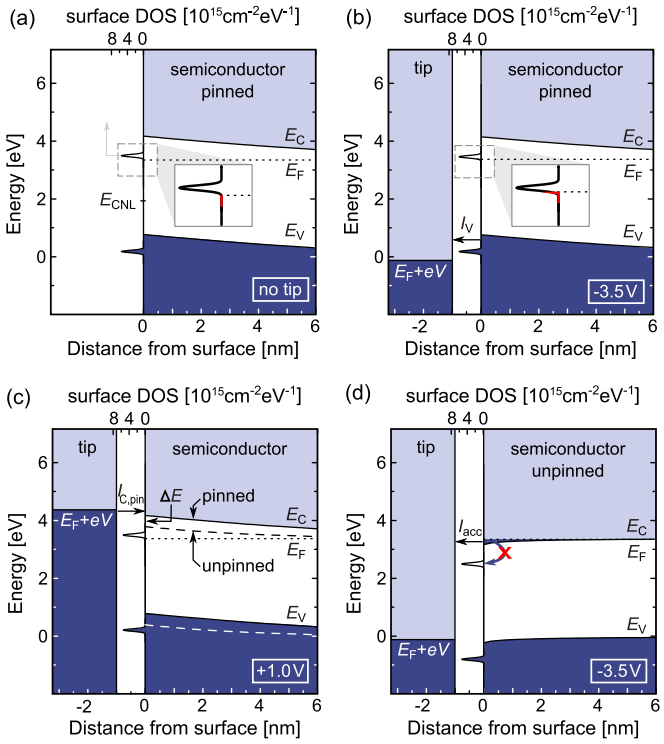


FIG. 3. (Color online) Calculated valence ($E_{\mathrm{V}}$) and conduction ($E_{\mathrm{C}}$) band edge positions for a GaN surface with a filled and an empty intrinsic surface state. Their density of states is modeled as Gaussian distributions and given on the top axis. Following band-structure calculations [23] the upper (empty) intrinsic surface state is assumed to be 0.7 eV below the conduction-band minimum, whereas the lower one is below the valence-band edge. The same color and labeling conventions as in Fig. 2 are used. Four different configurations are shown: (a) Surface without tip and no applied voltage in equilibrium. The intrinsic surface state is partially occupied (see the tiny red area in the enlarged inset), fully pinning the surface and hence inducing an upward band bending. (b) Surface in the presence of the metallic tip with a negative sample voltage of −3.5 V. The system reaches equilibrium by partially occupying the surface state (see inset). This induces an upward band bending and fully pins the Fermi level. Hence, no electron accumulation in the conduction band exists and only electrons from the valence band tunnel ($I_{\mathrm{V}}$). (c) Surface biased at +1.0 V with the tip present. The system is again in equilibrium by partially filling the surface state and thus pinning the Fermi level. The band edge positions are presented by solid lines. For comparison, the band edge positions without surface state taken from Fig. 2(b) are shown as dashed lines. The bands are shifted by $\Delta E$, resulting in an offset of the onset voltage of the conduction-band tunnel current $I_{\mathrm{C}}$ as experimentally observed. (d) Nonequilibrium case of the tip-vacuum-semiconductor system with the semiconductor surface biased at −3.5 V. Under tunneling conditions the surface state does not reach its equilibrium filling, since the optical electron transition between the conduction band and the surface state is prohibited. Hence, there is no Fermi level pinning. This situation is observed experimentally.

is much smaller than that of the conduction-band edge, and indeed, experimentally, the surface state could only be detected at extremely small tip-sample separations [23]. Therefore we do not consider tunneling in/out of the intrinsic surface state.

At this stage we discuss which of the models describes the system properly. The best fit is obtained for an *unpinned* surface at *negative* voltages (red solid line in Fig. 1), but a *pinned* surface at *positive* voltages (blue solid line). This result indicates the existence of a voltage-dependent intrinsic pinning. What is the physical origin of this astonishing situation?

Due to the presence of an intrinsic surface state in the band gap, the central question is why the surface state does not affect the electrostatic potential distribution at negative voltages. We recall that a completely empty surface state (neutral surface) does not influence the Fermi level. Hence, the above suggested lack of Fermi level pinning at negative voltages indicates that the surface state remains unoccupied, although it is shifted by band bending below the Fermi energy. *In equilibrium* the surface state would be filled at negative voltages [effect of pinning shown schematically in Fig. 3(b)]. However, under tunneling conditions the situation is different and the system is not in equilibrium anymore: For *n*-type material, the electrons filling the surface state can only originate from the conduction band. If the rate of electron transfer from the conduction band into the surface state (charging process) is smaller than that of electrons tunneling out of the surface state (discharging process), the surface state cannot reach its equilibrium filling and does not (or only partially) pin. Hence, we estimate the transfer probabilities between the conduction-band minimum and the surface state on the basis of the quantum-mechanical selection rules: For optical transitions of electrons from the conduction band into the surface state the selection rules require that the orbital angular momentum changes by $\pm 1$ [32]. However, both the conduction-band minimum and the minimum of the surface state at the $\overline{\Gamma}$ point have the same *s*-type orbital character [22,23,33,34] and hence direct optical transitions between them are prohibited. Only inelastic transitions may occur, whose probabilities are, however, much smaller due to need of an additional particle (e.g., phonon) [35]. In this situation the surface state is emptied by the tunnel process more rapidly than it is refilled from the conduction band. As a result, the surface state cannot reach its equilibrium filling under tunneling conditions at negative voltages and can hence not cause any pinning effect. The resulting band diagram is shown in Fig. 3(d).

In contrast, at positive voltages no electrons are extracted from the surface (only electron injection occurs) and hence, even for small transition rates between the conduction band and the intrinsic surface state in the band gap, the surface state can reach its equilibrium filling, resulting in the band diagram in Fig. 3(c).

In conclusion, the surface state in the band gap of GaN($10\overline{1}0$) surfaces pins the Fermi level only at small positive voltages, but not at negative voltages. This polarity dependence of the Fermi level pinning arises from the low transition rate of electrons from the conduction band to the surface state, inhibiting the filling of the surface state when shifted below the Fermi energy by band bending. Thus, even if an intrinsic surface state is present within the fundamental band gap, it may not pin the Fermi level or only at one polarity. This work shows that one needs to consider the electron transition rates from and to the surface state and therewith the quantum numbers of the involved states to determine the pinning potential of intrinsic surface states in the band gap. Similar effects may occur at interfaces of electronic devices, e.g., interface misfit dislocation arrays in heteroepitaxy, interfaces with oxide semiconductors, between Si and nitride semiconductors, and at the footprint of heteroepitaxially grown semiconductor nanowires, as well as at semiconductor nanowire sidewall facets. In all cases the pinning potential of interface states in the band gap has a crucial influence on the device properties.

The authors thank R. Butté and N. Grandjean, LASPE, Ecole Polytechnique Fédérale de Lausanne, Switzerland, for providing the sample, K.-H. Graf for technical support, and the Deutsche Forschungsgemeinschaft for financial support under Grants No. Eb 197/5-1, No. Ei 788/2-1, and No. SFB 787 TP A4.

[1] J. Bardeen, Phys. Rev. **71**, 717 (1947).
[2] W. Mönch, in *Electronic Structure of Metal-Semiconductor Contacts*, edited by W. Mönch, Perspectives in Condensed Matter Physics Vol. 4 (Kluwer Academic Publishers, Dordrecht, 1990).
[3] W. Mönch, *Semiconductor Surfaces and Interfaces*, 3rd ed. (Springer, Berlin, 2001).
[4] J. Robertson, J. Vac. Sci. Technol. A **31**, 050821 (2013).
[5] Ph. Ebert, K. Urban, L. Aballe, C. H. Chen, K. Horn, G. Schwarz, J. Neugebauer, and M. Scheffler, Phys. Rev. Lett. **84**, 5816 (2000).
[6] J. Tersoff and D. R. Hamann, Phys. Rev. Lett. **50**, 1998 (1983).
[7] R. M. Feenstra, J. A. Stroscio, J. Tersoff, and A. P. Fein, Phys. Rev. Lett. **58**, 1192 (1987).
[8] J. A. Stroscio, R. M. Feenstra, and A. P. Fein, Phys. Rev. Lett. **58**, 1668 (1987).
[9] S. Landrock, Y. Jiang, K. H. Wu, E. G. Wang, K. Urban, and Ph. Ebert, Appl. Phys. Lett. **95**, 072107 (2009).
[10] P. H. Weidlich, R. E. Dunin-Borkowski, and Ph. Ebert, Phys. Rev. B **84**, 085210 (2011).
[11] D. V. Froelich, M. E. Lapeyre, J. D. Dow, and R. E. Allen, Superlattices Microstruct. **1**, 87 (1985).
[12] R. M. Feenstra and J. A. Stroscio, J. Vac. Sci. Technol. B **5**, 923 (1987).
[13] N. D. Jäger, E. R. Weber, K. Urban, and Ph. Ebert, Phys. Rev. B **67**, 165327 (2003).
[14] N. Ishida, K. Sueoka, and R. M. Feenstra, Phys. Rev. B **80**, 075320 (2009).
[15] H. Eisele and P. Ebert, Phys. Status Solidi RRL **6**, 359 (2012).
[16] L. Ivanova, S. Borisova, H. Eisele, M. Dähne, A. Laubsch, and Ph. Ebert, Appl. Phys. Lett. **93**, 192110 (2008).

[17] M. Bertelli, P. Löptien, M. Wenderoth, A. Rizzi, R. G. Ulbrich, M. C. Righi, A. Ferretti, L. Martin-Samos, C. M. Bertoni, and A. Catellani, Phys. Rev. B **80**, 115324 (2009).
[18] J. E. Northrup and J. Neugebauer, Phys. Rev. B **53**, R10477 (1996).
[19] D. Segev and C. G. Van de Walle, Europhys. Lett. **76**, 305 (2006).
[20] C. G. Van de Walle and D. Segev, J. Appl. Phys. **101**, 081704 (2007).
[21] H. Ye, G. Chen, Y. Wu, Y. Zhu, and S.-H. Wei, Phys. Rev. B **80**, 033301 (2009).
[22] M. Landmann, E. Rauls, W. G. Schmidt, M. D. Neumann, E. Speiser, and N. Esser, Phys. Rev. B **91**, 035302 (2015).
[23] L. Lymperakis, P. H. Weidlich, H. Eisele, M. Schnedler, J.-P. Nys, B. Grandidier, D. Stievenard, R. E. Dunin-Borkowski, J. Neugebauer, and Ph. Ebert, Appl. Phys. Lett. **103**, 152101 (2013).
[24] P. H. Weidlich, M. Schnedler, H. Eisele, R. Dunin-Borkowski, and Ph. Ebert, Appl. Phys. Lett. **103**, 142105 (2013).
[25] Ph. Ebert, L. Ivanova, S. Borisova, H. Eisele, A. Laubsch, and M. Dähne, Appl. Phys. Lett. **94**, 062104 (2009).
[26] M. Himmerlich, A. Eisenhardt, S. Shokhovets, S. Krischok, J. Räthel, E. Speiser, M. D. Neumann, A. Navarro-Quezada, and N. Esser, Appl. Phys. Lett. **104**, 171602 (2014).
[27] N. D. Jäger, M. Marso, E. R. Weber, K. Urban, and Ph. Ebert, Phys. Rev. B **67**, 165307 (2003).
[28] Ph. Ebert, L. Ivanova, and H. Eisele, Phys. Rev. B **80**, 085316 (2009).
[29] R. M. Feenstra, Phys. Rev. B **50**, 4561 (1994).
[30] M. Schnedler, V. Portz, R. E. Dunin-Borkowski, and Ph. Ebert (unpublished).
[31] R. M. Feenstra, J. Vac. Sci. Technol. B **21**, 2080 (2003).
[32] W. C. Martin and W. L. Wiese, in *Atomic, Molecular, and Optical Physics Handbook* (American Institute of Physics, Melville, NY, 1996), pp. 135–153.
[33] W. G. Schmidt (private communication); the minimum of the empty surface state at the $\overline{\Gamma}$ point has a predominantly orbital character, whereas at the edge of the Brillouin zone the orbital character is predominantly $p$-type.
[34] S. Nakamura, S. Pearton, and G. Fasol, in *The Blue Laser Diode: The Complete Story* (Springer, New York, 2000), p. 34.
[35] V. N. Abakumov, V. I. Perel, and I. N. Yassievich, *Nonradiative Recombination in Semiconductors*, Modern Problems in Condensed Matter Sciences Vol. 33 (North Holland, Amsterdam, 1991).